Role of Active-Site Residues Thr81, Ser82, Thr85, Gln157, and Tyr158 inYeast Cystathionine β-Synthase Catalysis and Reaction Specificity†

Susan M. Aitken and Jack F. Kirsch*

Molecular and Cell Biology Department, University of California−Berkeley, Berkeley, California 94720-3206

Received August 21, 2003; Revised Manuscript Received November 6, 2003

ABSTRACT: Cystathionine β-synthase (CBS) effects the condensation of L-serine with L-homocysteine to form L-cystathionine. A series of active-site mutants, T81A, S82A, T85A, Q157A/E/H, and Y158F, was constructed to investigate effects on catalysis and reaction specificity in yeast CBS (yCBS). The effects of these mutations on the k_{cat}/K_m^{L-Ser} for the β-replacement reaction range from a reduction of only 3-fold for Y158F to below detectable levels for the Q157A and Q157E mutants. The order of importance of these residues to the β-replacement reaction is Gln157 ≥ Thr81 > Ser82 > Thr85 ≈ Tyr158. All seven of the mutant enzymes catalyze a competing β-elimination reaction, in which L-Ser is hydrolyzed to NH_3 and pyruvate. The ping-pong mechanism of CBS was thus expanded to include the latter reaction for these mutants. This activity is not detectable for wild-type yCBS, suggesting that the mutations result in a shift in the equilibrium between the open and the closed conformations of the active site of yCBS−substrate complexes. The Q157H and Y158F mutants additionally suffer suicide inhibition via a mechanism in which the released aminoacrylate intermediate covalently attacks the internal aldimine of the enzyme.

Cystathionine β-synthase (CBS)[1] catalyzes the pyridoxal 5′-phosphate-(PLP) dependent β-replacement reaction in which the hydroxyl group of L-Ser is displaced by the thiol of L-homocysteine (L-Hcys) to form L-cystathionine (L-Cth) (Scheme 1). This reaction comprises the first step in the transsulfuration pathway, which prevents the accumulation of L-Hcys by conversion of this toxic metabolite to L-Cys. Elevated plasma concentration of L-Hcys caused by mutations in the gene encoding human CBS (hCBS) is the major cause of homocystinuria, a disease with clinical manifestations that include vascular occlusions, skeletal abnormalities, and dislocation of the eye lens (*1*−*4*). Mammalian CBS is unique in that it is the only known enzyme to contain both PLP and heme (*5*). A regulatory role was proposed for the latter (*6*, *7*).

Scheme 1: CBS β-Replacement Reaction

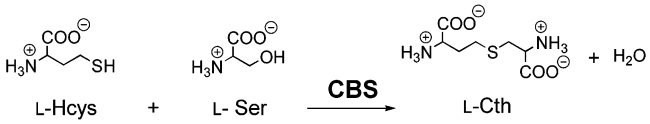

hCBS is prone to aggregation, and a truncated form of the enzyme, comprising the catalytic domain, which contains both the PLP and the heme cofactors, but not the C-terminal regulatory domain (residues 414−551), has proven more tractable for biophysical studies and crystallography (*7*, *8*). The overlapping absorbances of the PLP and heme cofactors of hCBS complicate the spectroscopic investigation of coenzyme-associated intermediates of the PLP, precluding presteady-state kinetics as a tool for mechanistic studies of CBS. Conveniently, yeast CBS (yCBS), which catalyzes the same reaction as hCBS, lacks the heme cofactor and the heme-binding domain (*9*, *10*). There is as yet no crystal structure of yCBS; however, the catalytic domain is 47% identical to that of hCBS, for which two structures are available (*7*, *8*), and the active-site residues are completely conserved. Therefore, yCBS is a useful model for investigation of the PLP-associated reactions of hCBS (*11*−*13*).

The β-replacement reactions catalyzed by tryptophan synthase (TrpS) and *O*-acetylserine sulfhydrylase (OASS) have been extensively studied (*14*, *15*). The latter enzyme is the closest homologue of CBS. The catalytic core of these two enzymes is so similar (1.32 Å rmsd) that the crystal structure of hCBS was solved by molecular replacement with the OASS structure from *Salmonella typhimurium* (*8*). The

† This work was supported by NIH Grant GM35393. S.M.A. was supported by a Heart and Stroke Foundation of Canada postdoctoral fellowship.

* To whom correspondence should be addressed. Telephone: (510) 642-6368. Fax: (510) 642-6368. E-mail: jfkirsch@uclink.berkeley.edu.

[1] Abbreviations: AA, aminoacrylate; AATase, aspartate aminotransferase; CBL, cystathionine β-lyase; CBS, cystathionine β-synthase; hCBS, human CBS; yCBS, yeast CBS; ytCBS, truncated yCBS (residues 1−353); L-Cth, L-cystathionine; DTNB, 5,5′-dithio-bis-(2-nitrobenzoic acid); EDTA, ethylenediaminetetraacetic acid; L-Hcys, L-homocysteine; k_{catF}/K_{mF}^{L-Ser}, the specificity constant, where the superscripts L-Ser, L-Hcys, and L-Cth refer to the substrate, and the reaction monitored is denoted by the subscript, where F, R, and E correspond to the forward β-replacement (L-Ser + L-Hcys → L-Cth), reverse β-replacement (L-Cth → L-Ser + L-Hcys), and β-elimination reactions (L-Cth → L-Hcys + pyruvate + NH_3 or L-Ser → pyruvate + NH_3), respectively; $K_{d(app)}^{L-Ser}$, the apparent dissociation constant for the E-AA complex due to L-Ser association with free enzyme; K_{iF1}^{L-Hcys}, the E-Hcys dissociation constant; K_{iF2}^{L-HCYS}, the dissociation constant for the E-Ser-Hcys complex due to L-Hcys association with the E-Ser form of the enzyme before the aminoacrylate (AA) can be formed; LDH, L-lactate dehydrogenase; Ni-NTA, nickel-nitrilotriacetic acid; OASS, *O*-acetylserine sulfhydrylase; PCR, polymerase chain reaction; PLP, pyridoxal 5′-phosphate; TrpS, tryptophan synthase.

10.1021/bi035496m CCC: $27.50
Published on Web 01/27/2004

Table 1: Primers Used in This Study[a]

name	sequence
BamHI	CAATCCAGGTGGATCCATCAAAGACAGAATTGCC
pSECseq0	GGCGTCAGGCAGCCATCGGAAGCTG
pSECseq1	CGGTTCTGGCAAATATTCTGAAATGAGCTG
PSECseq4r	CAGAACCGGAAGAACCACCCACCAAGACAC
ytCBShisC	TTCCAATGCATTGGCTGCAGTTA**ATGGTGGTGATGGTGGTG**CAGCTTTGAAGAGTCAAAACGGGCC
T81A	CTCTGATCGAACCT**GCT**TCTGGTAACACCG
S82A	CTCTGATCGAACCTACT**GCT**GGTAACACCG
T85A	CGAACCTACTTCTGGTAAC**GCT**GGTATCGGTC
Q157A	GCTGTTATACTTGAC**GCT**TATAACAATATGATG
Q157H	GCTGTTATACTTGAC**CAT**TATAACAATATGATG
Q157E	GCTGTTATACTTGAC**GAA**TATAACAATATGATG
Y158F	GCTGTTATACTTGACCAA**TTC**AACAATATGATG

[a] Names of mutagenic primers refer to the mutated amino acid position and are given only for the forward primer. The mutated codons and the His-tag are in bold, and introduced restriction sites are underlined.

K41A mutant of the active-site lysine residue of OASS, which is covalently linked to PLP as the internal aldimine in the wild-type enzyme, is purified as the external aldimine of L-methionine (*16*, *17*). The crystal structure of this mutant confirmed that a conformational change occurs upon substrate binding as, in contrast to the native enzyme, the active site of the K41A-L-Met complex is in the closed conformation and can therefore serve as a model of the substrate external aldimine. The carboxylate group of the external aldimine of L-Met forms a series of H-bonds to residues Pro67-Thr68-Asn69-Gly70 of OASS, referred to as the asparagine loop. The rearrangement of this loop in the active site induces a larger conformational change in the protein, where a subdomain undergoes a rigid-body rotation toward the active site, resulting in restricted access to the active site and protection from the bulk solvent (*17*). The side chains of Thr68, Asn69, Thr72, and Gln142 of OASS, which correspond to Thr81, Ser82, Thr85, and Gln157 in yCBS (yCBS numbering is employed for both CBS and OASS from this point forward unless specified otherwise), are all less than 3.2 Å from the carboxylate oxygen atoms of the bound L-Met (Scheme 2). Therefore, the T81A, S82A, T85A, Q157A, Q157E, and Q157H mutants were constructed in yCBS to probe the specific roles of these residues. Tyr158 (Y158F) was also selected for investigation, as the corresponding residue in hCBS (Tyr223) was proposed to be a determinant of substrate specificity (*8*).

Scheme 2: Proposed Active Site Contacts in the yCBS-L-Met External Aldimine Complex[a]

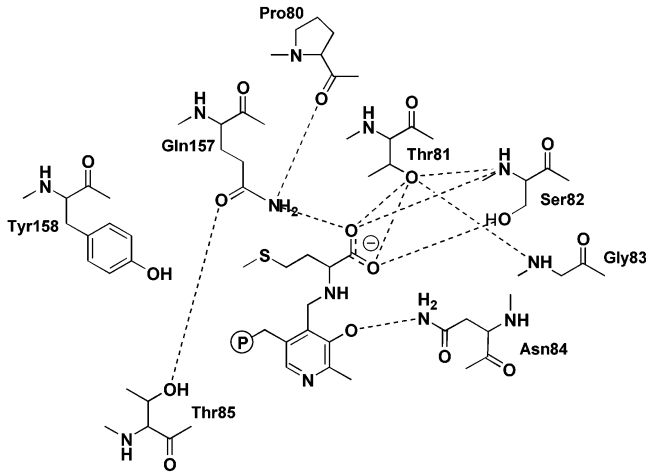

[a] The dotted lines represent putative distances of ≤3.2 Å between heteroatoms in yCBS, based on the structure of the OASS(K41A)-L-Met complex (*17*), which includes some H-bonds. Residue labels are those of yCBS where Thr81^{yCBS} ↔ Thr68^{OASS}, Ser82^{yCBS} ↔ Asn69^{OASS}, Gly83^{yCBS} ↔ Gly70^{OASS}, Asn84^{yCBS} ↔ Asn71^{OASS}, Thr85^{yCBS} ↔ Thr72^{OASS}, Gln157^{yCBS} ↔ Gln142^{OASS}, and Y158^{yCBS} ↔ F143^{OASS}.

EXPERIMENTAL PROCEDURES

Reagents. L-Cth [(*R*)-*S*-(2-amino-2-carboxyethyl)-L-homocysteine] and L-Ser were purchased from Fluka. L-Lactate dehydrogenase (LDH) and L-Hcys thiolactone were obtained from Sigma. L-Hcys was prepared from the thiolactone (*18*). Protease inhibitor (Complete EDTA-free) tablets were a Roche product. Nickel-nitrilotriacetic acid (Ni-NTA) resin was from Qiagen, and 5,5′-dithio-bis-(2-nitrobenzoic acid) (DTNB) was from Pierce. His-tagged cystathionine β-lyase (CBL) was expressed and purified as described previously (*13*).

Site-Directed Mutagenesis. A unique, silent BamHI site was introduced at position 149 of the gene encoding truncated yCBS (ytCBS) by recombinant polymerase chain reaction (PCR), employing the BamHI (and its inverse complement), pSECseq0, and pSECseq4r (Table 1) oligonucleotides (*19*). The amplification product was digested with Eco81I and NruI and cloned into the corresponding sites of the pT-SEC vector to produce the modified construct, pT-SECb, which was transformed into the *Escherichia coli* strain DH10B (Gibco BRL) via electroporation (Gene Pulser, BioRad). A portion of the pT-SECb plasmid, from 163 to 1323 bp, was subsequently PCR amplified with the pSECseq1 and ytCBShisC primers (Table 1). The latter primer introduces a C-terminal, six-His tag and a PstI restriction site. The amplification product was digested with BamHI and PstI, cloned into the corresponding sites of the pT-SECb vector, and transformed into *E. coli* strain DH10B as described above. The resulting construct is referred to as pTSECb-His. Mutations were introduced into ytCBS-His by the method described above (*19*) for the incorporation of the silent BamHI site, with pSECseq1 and ytCBShisC as the 5′ and 3′ flanking primers, respectively. The sequences of the mutagenic primers employed are given in Table 1.

Expression and Purification of ytCBS-His. The growth conditions for the overexpression of ytCBS-His were

described previously (*13*, *20*). The harvested cell pellet was suspended in 100−150 mL of buffer A (50 mM K phosphate, pH 7.8, 10 mM β-mercaptoethanol, and 10 mM imidazole) containing one Complete EDTA-free tablet (Roche) and 20 μg/mL DNAse I. The cells were disrupted by incubation with 1 mg/mL lysozyme on ice for 20 min followed by repeated (8 × 30 s) cycles of sonication (Misonix 3000 sonicator) at a power setting of 30 W. The lysate was centrifuged, the supernatant was loaded onto a 1.5 × 10 cm column of Ni-NTA resin (Qiagen), and the column was washed with 200 mL of buffer A. The enzyme was eluted with a 400 mL linear gradient of 10−400 mM imidazole in buffer A. The ytCBS-His-containing fractions were pooled, concentrated, and dialyzed against storage buffer (50 mM potassium phosphate, pH 7.8, 1 mM EDTA, 1 mM DTT, 20 μM PLP). At least 70 mg of ≥95% pure ytCBS-His (wild-type and mutants) was obtained from a 3 L culture.

Steady-State Kinetics. CBS β-elimination and β-replacement activities were assayed by the continuous LDH and CBL-LDH assays, in which formation of pyruvate and l-Cth, respectively, are monitored continuously (*13*). The DTNB assay was employed to monitor the hydrolysis of L-Cth to L-Ser and L-Hcys (*13*). The kinetic parameters for the β-replacement reaction of ytCBS and ytCBS-His were determined from the fit of the data to eq 1, where $F_1^{\text{L-Hcys}} = 1 + [\text{L-Hcys}]/K_{\text{iF1}}^{\text{L-Hcys}}$ and $F_2^{\text{L-Hcys}} = 1 + [\text{L-Hcys}]/K_{\text{iF2}}^{\text{L-Hcys}}$ (*20*).

$$\frac{v}{[\text{E}]} = [k_{\text{catF}}[\text{L-Ser}][\text{L-Hcys}]]/[K_{\text{m}}^{\text{L-Hcys}}F_1^{\text{L-Hcys}}[\text{L-Ser}] + K_{\text{m}}^{\text{L-Ser}}[\text{L-Hcys}] + F_2^{\text{L-Hcys}}[\text{L-Ser}][\text{L-Hcys}]] \quad (1)$$

The kinetic parameters for the β-elimination and reverse reaction were determined from the fit of the data to the Michaelis−Menten equation, and $k_{\text{cat}}/K_{\text{m}}$ was obtained independently from eq 2.

$$\frac{v}{[\text{E}]} = \frac{\frac{k_{\text{catR}}}{K_{\text{m}}^{\text{L-Cth}}}[\text{L-Cth}]}{1 + \frac{[\text{L-Cth}]}{K_{\text{m}}^{\text{L-Cth}}}} \quad (2)$$

Determination of $K_{\text{d(app)}}^{\text{L-Ser}}$. Fluorescence spectra were acquired with a Perkin-Elmer model LS-50B spectrofluorimeter at 37 °C. The apparent dissociation constant for the E-AA complex due to L-Ser association with free enzyme ($K_{\text{d(app)}}^{\text{L-Ser}}$) was determined by the protocol described by Jhee et al. (*20*), where 1.0 μM ytCBS, wild-type or mutants, was titrated with aliquots of L-Ser, and the increase in fluorescence at 540 nm (λ_{ex} = 460 nm) due to formation of the aminoacrylate (AA) intermediate was monitored. The change in fluorescence at 540 nm was plotted versus [L-Ser] and fit to eq 3 (*20*).

$$\Delta F = \frac{\Delta F_{\text{max}}[\text{L-Ser}]}{K_{\text{d}} + [\text{L-Ser}]} \quad (3)$$

Absorption spectra were acquired with a Hewlett-Packard model 8453 diode array spectrophotometer at 37 °C. Spectra were recorded for 20 μM ytCBS-His, wild-type and mutants, in the presence of 50 mM L-Ser or 4 mM L-Cth.

Single-Turnover Measurements. The reaction of 20 μM Y158F with 4 mM L-Cth in 50 mM Tris, pH 8.6, 5 μM PLP was monitored at 320 and 460 nm over the course of 2.5 h, and the data were fit to eqs 4 and 5, respectively.

$$A_{320} = A_{\text{max}} - \Delta A e^{-k_{\text{obs}}t} \quad (4)$$

$$A_{460} = A_{\text{min}} + \Delta A e^{-k_{\text{obs}}t} \quad (5)$$

The reaction of 20 μM Q157H with 2.5−400 mM L-Ser in 50 mM Tris, pH 8.6, 2.5 μM PLP at 37 °C was monitored at 320 nm during the first 2.5 h of the reaction, and the data were fit to eq 4. The resulting k_{obs} values were plotted versus [L-Ser] and fit to eq 6 to obtain k_{max} and apparent K_{m} ($K_{\text{m}}^{\text{app}}$) values.

$$k_{\text{obs}} = \frac{k_{\text{max}}[\text{L-Ser}]}{K_{\text{m}}^{\text{app}} + [\text{L-Ser}]} \quad (6)$$

The formation of the AA intermediate (460 nm) of T81A and ytCBS upon reaction with L-Ser (0.25−30 mM for ytCBS and 2.5−250 mM for T81A) was monitored at 460 nm with a stopped-flow spectrophotometer (Applied Photophysics Ltd. SF.17MV). Data were collected at 460 nm during the first 0.2 and 40 s for ytCBS and T81A, respectively. Values of k_{max} and $K_{\text{m}}^{\text{app}}$ were determined as described for Q157H.

RESULTS

Nickel Affinity Column Chromatography of ytCBS-His and Comparison with Untagged Enzyme. Purification of wild-type and mutant ytCBS was facilitated by the addition of a C-terminal 6-histidine tag (ytCBS-His). The kinetic parameters for ytCBS-His were determined to ensure that the His-tag does not interfere with the activity of the enzyme (Table 2). The variation in all kinetic parameters is ≤2-fold between ytCBS and ytCBS-His, and the $k_{\text{catF}}/K_{\text{mF}}^{\text{L-Ser}}$ and $k_{\text{catF}}/K_{\text{mF}}^{\text{L-Hcys}}$ values (where the F subscript denotes kinetic parameters of the β-replacement reaction of Scheme 3) are equal within experimental error.

T85A and Y158F. The rate of formation of pyruvate from L-Ser and from L-Cth via β-elimination activity by these mutants was measured. In contrast to wild-type ytCBS, for which this activity is not detectable (Table 2), pyruvate production was observed for T85A ($k_{\text{catE}}^{\text{L-Ser}}/K_{\text{mE}}^{\text{L-Ser}}$ = 560 M^{-1} s^{-1} and $k_{\text{catE}}^{\text{L-Cth}}/K_{\text{mE}}^{\text{L-Cth}}$ = 70 M^{-1} s^{-1}, where the E subscript denotes kinetic parameters of the β-elimination reaction) and for Y158F ($k_{\text{catE}}^{\text{L-Ser}}/K_{\text{mE}}^{\text{L-Ser}}$ = 90 M^{-1} s^{-1} and $k_{\text{catE}}^{\text{L-Cth}}/K_{\text{mE}}^{\text{L-Cth}}$ = 13 M^{-1} s^{-1}). Therefore, the AA intermediates formed by T85A and Y158F dissociate from the enzyme, and the mechanism cannot be reduced to simple ping-pong kinetics in the forward direction. Eqs 7−9 were derived for the model shown in Scheme 3, which incorporates the two forms of substrate inhibition by L-Hcys (*20*) into a modified ping-pong mechanism in which the AA intermediate can either decay to release

Table 2: Steady-State Kinetic Parameters for ytCBS, ytCBS-His, and the T81A, S82A, and T85A Mutants[a]

	ytCBS[b]	ytCBS-His	T81A	T81A/ ytCBS-His[c]	S82A	S82A/ ytCBS-His[c]	T85A	T85A/ ytCBS-His[c]
				L-serine + L-homocysteine → L-cystathionine				
k_{catF} (s^{-1})[d]	21.5 ± 0.9	17 ± 1	0.45 ± 0.05	0.026	5.3 ± 0.5	0.31	13.2 ± 0.7	0.78
k_{catF}/K_{mF}^{L-Ser} (M^{-1} s^{-1})[d]	(1.8 ± 0.1) × 10^4	(2.5 ± 0.6) × 10^4	3.2 ± 0.4	0.00013	330 ± 30	0.014	6100 ± 900	0.25
k_{catF}/K_{mF}^{L-Hcys}(M^{-1} s^{-1})[d]	(7.9 ± 0.4) × 10^4	(8 ± 1) × 10^4	2100 ± 400	0.026	(2.0 ± 0.5) × 10^4	0.25	(1.6 ± 0.1) × 10^4	0.20
K_{iF1}^{L-Hcys} (mM)[d]	2.0 ± 0.4	1.0 ± 0.4			4 ± 3	4	1.8 ± 0.4	1.8
K_{iF2}^{L-Hcys} (mM)[d]	18 ± 4	15 ± 7	4.0 ± 0.7	0.27	11 ± 4	0.73	16 ± 3	1.1
$K_{d(app)}^{Ser}$ (μM)[e]	14 ± 0.25[g]	13.9 ± 0.4	(2.8 ± 0.2) × 10^4	2000	920 ± 50	67	13.8 ± 0.6	0.99
				L-serine → pyruvate + NH_3				
k_{catE}^{L-Ser} (s^{-1})[f]	<0.001	<0.001	0.0051 ± 0.0002		0.0208 ± 0.0007		0.073 ± 0.002	
$k_{catE}^{L-Ser}/K_{mE}^{L-Ser}$ (M^{-1} s^{-1})[f]	n.a.	n.a.	0.09 ± 0.01		16 ± 1		560 ± 90	
				L-cystathionine → L-homocysteine + L-serine				
k_{catR} (s^{-1})[f]	0.56 ± 0.01	1.03 ± 0.02	n.s.		0.083 ± 0.001	0.081	0.133 ± 0.001	0.13
k_{catR}/K_{mR}^{L-Cth} (M^{-1} s^{-1})[f]	6700 ± 200	7500 ± 400	0.8 ± 0.2	0.00011	80 ± 2	0.011	540 ± 20	0.072
				L-cystathionine → L-homocysteine + pyruvate + NH_3				
k_{catE}^{L-Cth} (s^{-1})[f]	<0.001	<0.001	<0.001		<0.001		0.035 ± 0.002	
$k_{catE}^{L-Cth}/K_{mE}^{L-Cth}$ (M^{-1} s^{-1})[f]	n.a.	n.a.	n.a.		n.a.		70 ± 10	

[a] n.a.: no detectable activity. n.s.: no saturation detected at [L-Cth] < 4 mM. [b] From ref *13*. [c] The values in this column give the *x*-fold change in the parameter with respect to wild-type ytCBS-His. [d] Kinetic measurements were carried out in 50 mM Tris, pH 8.6, containing 20 μM PLP at 37 °C. β-replacement conditions: 0.4 μM CBL, 1.3 μM LDH, 150 μM NADH, 0.025−15 mM L-Hcys, 0.05−180 mM L-Ser, and 0.026−25 μM ytCBS or mutant enzymes. β-replacement data for ytCBS and ytCBS-His were fit to eq 1, and those for the mutants were fit to eqs 7−9. The F subscript denotes kinetic parameters of the β-replacement reaction. [e] $K_{d(app)}^{L-Ser}$ values were determined by the increase in fluorescence at 540 nm (λ_{ex} = 460 nm), due to the formation of AA, resulting from a titration of 1.0 μM ytCBS-His, wild-type, and mutants, with aliquots of L-Ser (*20*). Data were fit to eq 3. [f] Data were fit to the Michaelis−Menten equation and eq 2. The E and R subscripts denote kinetic parameters of the β-elimination and reverse reactions, respectively. Hydrolysis of L-Cth to L-Ser and L-Hcys conditions: 2 mM DTNB, 0.015−4 mM L-Cth, and 0.64 μM ytCBS or mutant enzymes. [g] From ref *20*.

NH_3 and pyruvate or react with L-Hcys.

$$\frac{v}{[E]} = \left[K_{catE}[\text{L-Ser}] + \frac{K_{catF}}{K_{mF}^{L-Hcys}}[\text{L-Ser}][\text{L-Hcys}]\right] \Big/ \left[K_{mE}^{L-Ser} + [\text{L-Ser}] + \frac{K_{mF}^{L-Ser}}{K_{mF}^{L-Hcys}}F_1^{L-Hcys}[\text{L-Hcys}] + \frac{1}{K_{mF}^{L-Hcys}}F_2^{L-Hcys}[\text{L-Ser}][\text{L-Hcys}]\right] \quad (7)$$

F_1^{L-Hcys} and F_2^{L-Hcys} are defined above eq 1. The data obtained for T85A in the CBL/LDH coupled assay for the β-replacement reaction were fit to eq 7 to obtain k_{catE} (0.1 ± 0.2 s^{-1}) and K_{mE}^{L-Ser} (0.5 ± 0.3 mM). Despite the large error in these values, they are close to those determined directly in the absence of L-Hcys (Table 2), demonstrating that the presence of L-Hcys does not significantly influence the rate of the elimination reaction. The values of k_{catE} and K_{mE}^{L-Ser}, determined via the elimination assay, were substituted into eqs 8 and 9, thereby reducing the number of kinetic parameters to be determined. The resulting fitted parameters for the replacement reaction are presented in Table 2. The terms in eq 7 were multiplied by K_{mF}^{L-Hcys} yielding eq 8, to which the T85A data were fit to obtain k_{catF}, K_{mF}^{L-Ser}, and K_{mF}^{L-Hcys} (*13*).

$$\frac{v}{[E]} = [k_{catE}K_{mF}^{L-Hcys}[\text{L-Ser}] + K_{catF}[\text{L-Ser}][\text{L-Hcys}]] / [K_{mE}^{L-Ser}K_{mF}^{L-Hcys} + K_{mF}^{L-Hcys}[\text{L-Ser}] + K_{mF}^{L-Ser}F_1^{L-Hcys}[\text{L-Hcys}] + F_2^{L-Hcys}[\text{L-Ser}][\text{L-Hcys}]] \quad (8)$$

The terms in eq 8 were divided by K_{mF}^{L-Ser} to yield eq 9, to which the data were fit to obtain k_{catF}/K_{mF}^{L-Ser}.

$$\frac{v}{[E]} = \left[\frac{k_{catE}K_{mF}^{L-Hcys}}{K_{mF}^{L-Ser}}[\text{L-Ser}] + \frac{k_{catF}}{K_{mF}^{L-Ser}}[\text{L-Ser}][\text{L-Hcys}]\right] \Big/ \left[\frac{K_{mE}^{L-Ser}K_{mF}^{L-Hcys}}{K_{mF}^{L-Ser}} + \frac{K_{mF}^{L-Hcys}}{K_{mF}^{L-Ser}}[\text{L-Ser}] + F_1^{L-Hcys}[\text{L-Hcys}] + \frac{1}{K_{mF}^{L-Ser}}F_2^{L-Hcys}[\text{L-Ser}][\text{L-Hcys}]\right] \quad (9)$$

The data from the CBL/LDH assay for Y158F were also fitted to eqs 7−9 (Table 3). The k_{catF}/K_{mF}^{L-Ser} values of T85A and Y158F mutants are each reduced by only 4-fold, as compared to the wild-type enzyme. This reduction is due to approximately equal magnitude changes in k_{catF} and K_{mF}^{L-Ser} values for both mutants. The $K_{d(app)}^{L-Ser}$ of T85A is identical to that of ytCBS (Table 2) and that of Y158F is increased by only 2-fold (Table 3). The K_{mF}^{L-Hcys} of T85A is 4-fold greater than that of the wild-type enzyme. This mutation is the only one of the seven investigated that elicited any effect on this kinetic parameter.

Both T85A and Y158F catalyze the hydrolysis of L-Cth to L-Ser and L-Hcys (Table 2). The k_{catR}/K_{mR}^{L-Cth} [where the R subscript denotes kinetic parameters of the reverse reaction (*13*)] for the hydrolysis of L-Cth to L-Hcys and L-Ser is reduced to the same degree (3-fold) as the k_{catF}/K_{mF}^{L-Ser} for the β-replacement reaction for Y158F, while k_{catR}/K_{mR}^{L-Cth} of T85A is reduced to a greater extent (14-fold) as compared to k_{catF}/K_{mF}^{L-Ser} (4-fold). The internal aldimine (412 nm) of

Table 3: Steady-State Kinetic Parameters for Q157A/E/H and Y158F Mutant Forms of ytCBS[a]

	Q157A	Q157A/ ytCBS-His[b]	Q157E	Q157E/ ytCBS-His[b]	Q157H	Q157H/ ytCBS-His[b]	Y158F	Y158F/ ytCBS-His[b]
				L-serine + L-homocysteine → L-cystathionine				
k_{catF} (s^{-1})[c]	n.a		n.a		0.082 ± 0.004	0.0048	8.2 ± 0.6	0.48
$k_{catF}/K_{mF}^{L\text{-}Ser}$ ($M^{-1}s^{-1}$)[c]	n.a		n.a		21 ± 1	0.00088	7000 ± 1000	0.29
$k_{catF}/K_{mF}^{L\text{-}Hcys}$ ($M^{-1}s^{-1}$)[c]	n.a.		n.a.		700 ± 200	0.0086	(3.0 ± 1.0) × 10^4	0.37
$K_{iF1}^{L\text{-}Hcys}$ (mM)[c]	n.a.		n.a.		n.a.		1.0 ± 0.3	1.0
$K_{iF2}^{L\text{-}Hcys}$ (mM)[c]					4.4 ± 0.6	0.29	20 ± 10	1.3
$K_{d(app)}^{L\text{-}Ser}$ (μM)[d]							30.6 ± 0.9	2.2
				L-serine → pyruvate + NH_3				
$k_{catE}^{L\text{-}Ser}$ (s^{-1})[e]	1.24 ± 0.09		0.73 ± 0.08		0.075 ± 0.005		0.0176 ± 0.0004	
$k_{catE}^{L\text{-}Ser}/K_{m}^{L\text{-}Ser}$ (M^{-1} s^{-1})[e]	6.2 ± 0.6		1.9 ± 0.1		0.39 ± 0.03		90 ± 10	
				L-cystathionine → L-homocysteine + L-serine				
k_{catR} (s^{-1})[e]	n.s.		n.s.		n.a.		0.418 ± 0.004	0.41
$k_{catR}/K_{mR}^{L\text{-}Cth}$ ($M^{-1}s^{-1}$)[e]	1.18 ± 0.07	0.00016	4.2 ± 0.2	0.00056	n.a.		1490 ± 60	0.20
				L-cystathionine → L-homocysteine + pyruvate + NH_3				
$k_{catE}^{L\text{-}Cth}$ (s^{-1})[e]	n.s.		0.0237 ± 0.0008		n.a.		0.0055 ± 0.0002	
$k_{catE}^{L\text{-}Cth}/K_{mE}^{L\text{-}Cth}$ ($M^{-1}s^{-1}$)[e]	1.05 ± 0.08		23 ± 2		n.a.		13 ± 2	

[a] n.a.: no detectable activity. n.s.: no saturation detected at [L-Cth] < 4 mM. [b] The values in this column give the *x*-fold change in the parameter with respect to wild-type ytCBS-His. [c] See footnote *d* of Table 2. [d] See footnote *e* of Table 2. [e] Data were fit to the Michaelis−Menten equation and eq 2. The E and R subscripts denote kinetic parameters of the β-elimination and reverse reactions, respectively.

Scheme 3: Kinetic Mechanism Describing the β-Elimination and β-Substitution Reactions Catalyzed by the ytCBS Mutants[a]

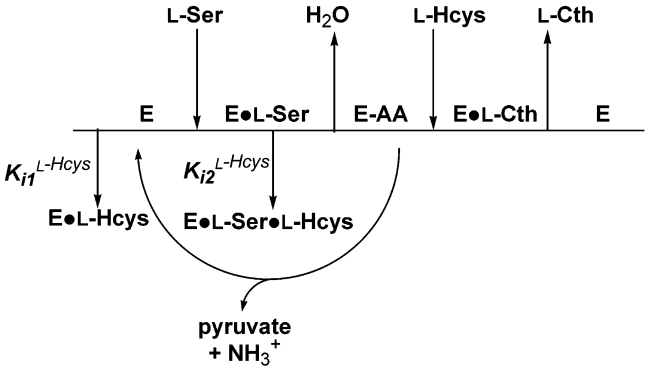

[a] L-Ser associates with the enzyme to form the external aldimine (E•L-Ser). H_2O is subsequently eliminated to form the aminoacrylate complex (E-AA). L-Hcys, when present, reacts with E-AA to form the external aldimine of L-Cth (E•L-Cth), from which L-Cth is released. Substrate inhibition (K_{i1}^{Hcys}) is due to competition by L-Hcys with L-Ser for the free enzyme (E), to form a nonproductive E-L-Hcys complex. A second form of substrate inhibition (K_{i2}^{Hcys}) arises from the binding of L-Hcys to the E•L-Ser complex prior to the release of H_2O. The AA complex is stable in wild-type ytCBS, but in the all of the mutants investigated, it can decompose to NH_3, pyruvate, and the internal aldimine form of the enzyme via the elimination reaction.

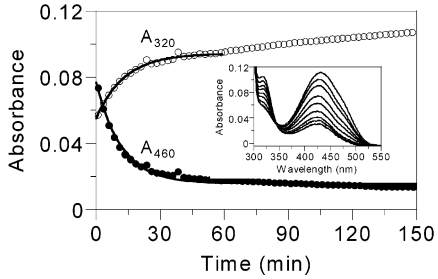

FIGURE 1: Time course of the reaction of the Y158F mutant of yeast truncated cystathionine β-synthase (ytCBS) with L-Cth. Absorbance was monitored at 460 nm (filled circles) and 320 nm (open circles) following the addition of 20 μM Y158F to 4 mM L-Cth in 50 mM Tris, pH 8.6, 2.5 μM PLP, at 37 °C. The lines represent fits to eqs 4 (320 nm) and 5 (460 nm). The linear increase in 320 nm absorbance, which is most apparent after 60 min, is due to the production of pyruvate, which absorbs in this region. Inset: time-resolved spectra of the above reaction at 0.5, 2, 4, 8, 12, 20, 45, 90, and 150 min.

Y158F is converted to a species absorbing at ~320 nm during the course of the 2.5 h incubation with L-Cth (Figure 1). The same trend is observed upon incubation (2.5 h) with L-Ser (data not shown).

T81A and S82A. These mutations result in more dramatic changes in the kinetic parameters of ytCBS than do T85A and Y158F. Since the T81A and S82A mutant enzymes both catalyze the hydrolysis of L-Ser to pyruvate and NH_3, the kinetic parameters for the β-replacement reaction of both mutants were determined by fitting the kinetic data to eqs 7−9. The k_{catF}/K_{mF}^{L-Ser} values of the T81A and S82A mutants are reduced by 7000- and 80-fold, respectively, as compared to the wild-type enzyme (Table 2). The k_{catF}/K_{mF}^{L-Ser} of the T81A mutant is dominated by the increase in K_{mF}^{L-Ser} (200-fold), although k_{catF} is also affected (40-fold reduction). The 2000-fold increase in the $K_{d(app)}^{L-Ser}$ value of T81A indicates that L-Ser binding is severely compromised by this mutation (Table 2). The decrease in k_{catF}/K_{mF}^{L-Ser} for S82A is also driven by an increase (20-fold) in K_{mF}^{L-Ser}, as k_{catF} is only reduced 3-fold. These results, combined with the observation that $K_{d(app)}^{L-Ser}$ is increased 70-fold, suggest a role for Ser82 in L-Ser binding. The k_{catR}/K_{mR}^{L-Cth} values of T81A and S82A are reduced by 9000- and 90-fold, respectively, as compared to ytCBS-His. The degree of reduction in k_{catR}/K_{mR}^{L-Cth} is almost identical to the reduction of the k_{catF}/K_{mF}^{L-Ser} for both mutant enzymes (Table 2). β-elimination activity was not detected for either mutant with L-Cth as a substrate.

As reported by Jhee et al. (*11*), the reaction of free enzyme (E) with L-Ser (Scheme 3) to form AA follows the sequence of eq 10.

$$E + L\text{-Ser} \underset{k_2}{\overset{k_1}{\rightleftharpoons}} E{\cdot}L\text{-Ser} \underset{k_{4*}}{\overset{k_3}{\rightleftharpoons}} E\text{-AA} \quad (10)$$

where $k_{4*} = k_4[H_2O]$ and $K_{21} = k_2/k_1$. The rates of AA formation of ytCBS at 37 °C versus L-Ser concentration (Figure 2) were fit to eq 11 (*11*).

$$k_{obs} = \frac{k_3[L\text{-Ser}]}{K_{21} + [L\text{-Ser}]} + k_{4*} \quad (11)$$

The values of k_3 (250 ± 5 s^{-1}) and K_{21} (2.4 ± 0.2 mM) for the wild-type enzyme are 2- and 0.5-fold, respectively, of those reported at 25 °C (*11*). In contrast, no saturation behavior was observed for the T81A mutant at [L-Ser] ≤250 mM (Figure 2); therefore, the data were fit to eq 12.

$$k_{obs} = \frac{k_3}{K_{21}}[L\text{-Ser}] + k_{4*} \quad (12)$$

The value of k_3/K_{21} is 3.52 ± 0.08 M^{-1} s^{-1}. This figure, which is 4 orders of magnitude lower than that of the wild-type enzyme, is very close to the k_{catF}/K_{mF}^{L-Ser} (3.2 ± 0.4 M^{-1} s^{-1}) determined for T81A (Table 2).

Gln157 Mutants. The kinetic parameters for the three Gln157 mutants are included in Table 3. L-Hcys (≤8 mM) had no observable effect on the activity of the Q157A and Q157E mutants, indicating that they do not catalyze the condensation of L-Ser and L-Hcys to form L-Cth. Although the β-replacement activity of the Q157H mutant was detectable, the k_{catF}/K_{mF}^{L-Ser} is reduced by 4 orders of magnitude as compared to the wild-type enzyme. The Gln157 mutants are not saturated by 4 mM L-Cth; therefore, only k_{catR}/K_{mR}^{L-Cth} could be determined. This activity was undetectable for Q157H and reduced by greater than 3 orders of magnitude for Q157A and Q157E. Only Q157A and Q157E exhibit detectable elimination activity from L-Cth.

Pyruvate formation in the Q157A-catalyzed β-elimination of L-Ser is also apparent in Figure 3, where the spectra of Q157A and Q157H following a 3 h incubation with 50 mM L-Ser are shown. The high absorbance at $\lambda < \sim$400 nm in the Q157A spectrum after 3 h is due to the high concentration (approaching 50 mM) of pyruvate, consistent with the activity observed for this mutant in the elimination assay. In contrast, there was much less pyruvate present after incubation with Q157H (Figure 3), which has a $k_{catE}^{L-Ser}/K_{mE}^{L-Ser}$ that is 16-fold lower than that of Q157A. The internal aldimine (412 nm) of Q157H is converted to a species absorbing at ~320 nm during the course of the 3 h incubation (Figure 4). The rate of formation of this species and the corresponding rate of decay of the 412 nm absorbance were determined for L-Ser concentrations from 2.5 to 400 mM, and the k_{obs} versus [L-Ser] data for [L-Ser] <100 mM were fit to eq 6 to yield k_{max} and K_m^{app} values of (4.3 ± 0.4) × 10^{-4} s^{-1} and 35 ± 9 mM, respectively (Figure 5). The error in these values is likely underestimated due to the inhibition of formation of the 320 nm species at concentrations of L-Ser ≥100 mM. The possibility that the 320 nm species results from attack by AA on the internal aldimine, as in the mechanism of aspartate aminotransferase (AATase) inactivation by L-serine-*O*-sulfate (*21*, *22*), was investigated. Following a 3 h incubation of 20 μM Q157H with 50 mM L-Ser, the remaining L-Ser was removed by dialysis in 5 mM Tris, pH 8.6. The spectrum of the enzyme was unchanged by the dialysis step. The pH was subsequently adjusted to 11.5, and the increase in absorbance at 424 nm, diagnostic of species **5** [4-[2-methyl-3-hydroxy-5-(phosphooxymethyl)-4-pyridinyl]-2-oxo-3-butenoic acid, Scheme 4 (*23*)] was observed. Therefore, the inactivation of the Q157H mutant enzyme by L-Ser likely follows the L-serine-*O*-sulfate mechanism (*21*, *22*).

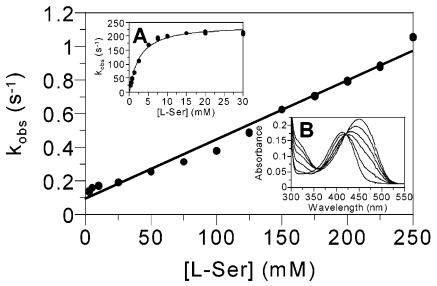

FIGURE 2: Dependence of the observed first-order rate constant (k_{obs}) on [L-Ser] for aminoacrylate formation by the T81A mutant. T81A (20 μM) was reacted with 2.5−250 mM L-Ser. The line represents the fit of the data to eq 12. Inset A: ytCBS-His (20 μM) was reacted with 0.25−30 mM L-Ser. The line represents the fit of the data to eq 11. Inset B: spectra of 20 μM T81A after 60 s incubation with 0, 10, 50, 75, 125, and 200 mM L-Ser. Conditions as in Figure 1.

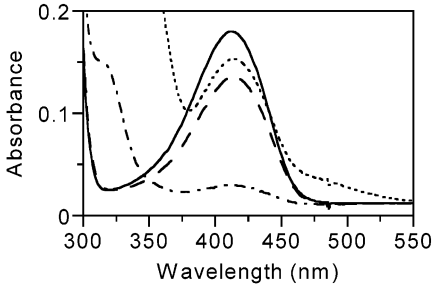

FIGURE 3: Spectra of 20 μM Q157A (—) and Q157H (- - -) alone and after 3 h incubation with 50 mM L-Ser (··· Q157A; -·-·- Q157H). Conditions as in Figure 1.

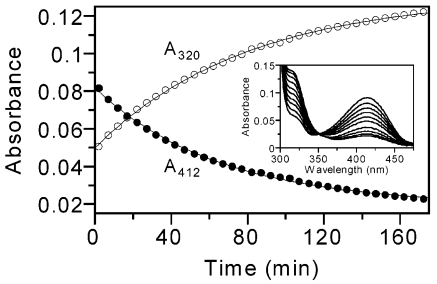

FIGURE 4: Time course of the reaction of Q157H with L-Ser. Absorbance was monitored at 412 nm (filled circles) and 320 nm (open circles) following the addition of 50 mM L-Ser to 20 μM Q157H. The lines represent fits to eqs 4 (320 nm) and 5 (412 nm). Inset: time-resolved spectra of the above reaction at 2, 10, 20, 30, 45, 60, 90, 120, 150, and 180 min. Conditions as in Figure 1.

DISCUSSION

CBS, a typical member of the β-replacement-specific PLP enzymes of the β-family (e.g., OASS and TrpS), does not possess an active-site arginine residue positioned to bind the carboxylate group of the first substrate, L-Ser (*7*, *8*). This contrasts with the much larger α-family (*24*) of PLP-dependent enzymes, including such diverse representatives

Scheme 4: β-Replacement, β-Elimination, and Inactivation Reactions Diverge from the Aminoacrylate Intermediate Formed from L-Ser[a]

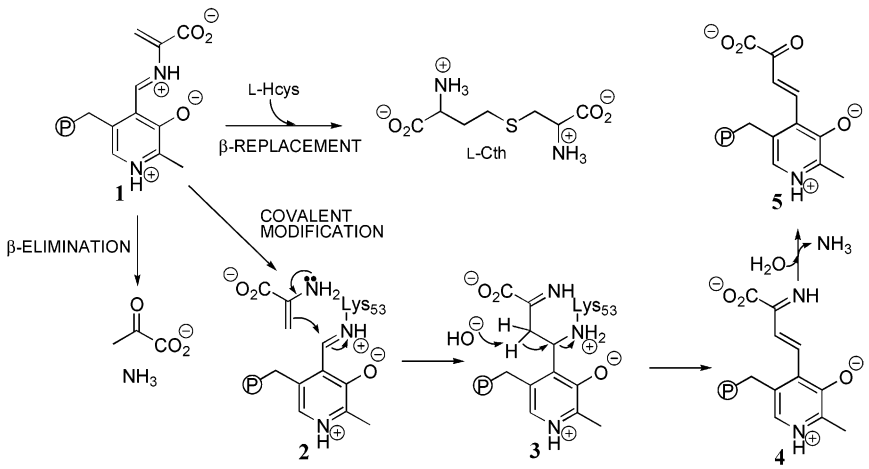

[a] The scheme for covalent modification of CBS is based on the mechanism for AATase inhibition by L-serine-*O*-sulfate (*21*, *22*) and for TrpS inhibition by β-chloro-L-alanine (*23*).

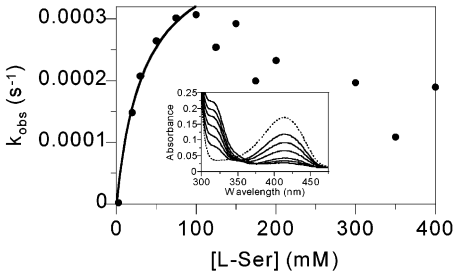

FIGURE 5: Dependence of the observed first-order rate constant (k_{obs}) for formation of the 320 nm absorbing species of Q157H on [L-Ser]. The enzyme (20 μM) was reacted with 2.5−400 mM L-Ser at 37 °C. The line represents the fit of the data to eq 6 for [L-Ser] < 100 mM. Inset: spectra of 20 μM Q157H alone (···) and after 3 h incubation (—) with 2.5, 5, 10, 20, 30, and 50 mM L-Ser in 50 mM Tris, pH 8.6.

as AATase (*25*), 1-aminocyclopropane-1-carboxylate synthase (*26*), cystathionine β-lyase (*27*), and cystathionine γ-synthase (*28*), which do employ such arginine anchors. The structure of inhibitor and substrate complexes of OASS and TrpS, respectively, show that the α-carboxylate group is bound at the active site by a hydrogen-bonding network (*17*, *29*). Several active-site residues form H-bonds with the carboxylate group of L-Met in the OASS/K41A-L-Met complex. Residues 67−72 and 142 in OASS (corresponding to Pro80-Thr81-Ser82-Gly83-Asn84-Thr85 and Gln157 of yCBS) comprise a network, some of whose members fulfill that function. Residues 67−70 of OASS also form the mobile loop that transitions between the open and the closed conformations of the active site. The AA intermediate of the β-replacement reaction is solvent reactive; therefore, it must be protected. This is accomplished by the conformational change observed in OASS (*17*). A similar conformational transition is expected in CBS because AA is an intermediate in the β-replacement reaction.

The active-site mutants of ytCBS (T81A, S82A, T85A, Q157A/E/H, and Y158F) were constructed to probe the roles of the parent residues in catalysis and as determinants of the reaction specificity of CBS. The results indicate that the order of importance of these residues in terms of their effects on the rate constants for the β-replacement reaction is Gln157 ≥ Thr81 > Ser82 > Thr85 ≈ Tyr158. It was found additionally that they all contribute to suppression of the undesired β-elimination reaction. This activity, which is undetectable in the wild-type enzyme, is catalyzed by all of the mutant enzymes. Furthermore, both the Y158F and the Q157H mutants form an inactivated enzyme species absorbing at 320 nm upon extended reaction with L-Ser or L-Cth. This 320 nm species does not arise in the wild-type enzyme.

Thr85 and Tyr158 Are Determinants of Reaction Specificity But Do Not Play a Major Role in the β-Replacement Reaction Kinetics. The side chain Oγ of Thr85 is 2.53 and 2.69 Å, respectively, from Gln157-Nϵ in the unliganded structures of hCBS and in OASS, while Thr85-Oγ is 3.69 and 2.82 Å from Nϵ and Oϵ, respectively, of Gln157 in the OASS/K41A-L-Met complex (*7*, *8*, *17*). Therefore, although Thr85 likely H-bonds to Gln157 in both the open and the closed conformations of OASS, the orientation of Gln157 is flipped such that the Thr85-Gln157 H-bond is to the Nϵ in the open form and to the Oϵ in the ligand-bound, closed form. The loss of the side chain hydroxyl group in the T85A mutant of ytCBS eliminates both of these H-bonds and therefore might differentially destabilize the open and closed conformations of the active site, resulting in a new equilibrium. While no β-elimination from either L-Ser or L-Cth is detectable with wild-type enzyme, this untoward side reaction occurs at approximately one tenth of the rate of the β-replacement reaction in T85A (Table 2). β-Elimination activity results from dissociation of the AA intermediate from the enzyme−AA complex. The $\alpha_2\beta_2$ form of TrpS also disfavors the β-elimination reaction, and the ratio of β-replacement to -elimination activity in the wild-type enzyme is 60 (*23*). Several mutants of the β-subunit of TrpS have been identified where this ratio is reduced. A shift in the equilibrium between the open and the closed forms of the enzyme has been proposed to account for the change in reaction specificity (*14*, *23*). Therefore, the β-elimination activity of the T85A mutant may indicate that the destabilizing effect of this mutation on the closed form is greater, thus shifting the equilibrium toward the open conformation. The effect of open versus closed conformation on reaction specificity has also been described for the well-studied PLP enzyme serine hydroxymethyltransferase (*30*). Since the T85A mutant, as well as the others investigated in this study,

exhibits both β-elimination and -replacement activities, the ping-pong mechanism of the wild-type enzyme was expanded (Scheme 3) to incorporate the former activity.

Tyr158 is conserved in yeast, human, rat, and mouse CBS as well as in a series of putative CBS sequences (rabbit, *Dictyostelium discoideum*, etc.) but is replaced by Phe in OASS. Tyr158 was proposed to be a determinant of the reaction specificity of hCBS based on the crystal structure (*8*). Tyr158 may be bridged by a water molecule to the backbone carbonyl of G245 in the hCBS structure. The latter corresponds to G305 in hCBS, and the G305R mutant is one of more than 90 linked to homocystinuria in humans (*4*). The active-site location of Tyr158, in combination with the conserved Phe replacement in OASS, suggests that it may be a determinant of substrate specificity. However, the k_{catF}/K_{mF}^{L-Ser} and k_{catF}/K_{mF}^{L-Hcys} of Y158F are each reduced by only 3-fold as compared to the wild-type enzyme, indicating that the hydroxyl group of Tyr158 is not a major factor in catalysis. The appearance of the elimination reaction for Y158F (Table 3) suggests that the hydroxyl group of Tyr158 apparently differentially stabilizes the closed conformation of the enzyme substrate complex, although to a lesser degree than does Thr85. The β-elimination activity of the Y158F mutant enzyme suggests that OASS, with a Phe residue at position 158, would have a similarly low partition ratio between the β-replacement and the β-elimination activities. However, the rate of the OASS-catalyzed β-elimination reaction is 10^4-fold slower than the β-replacement reaction (*31*).

Another partitioning pathway, in addition to β-replacement and -elimination, is found with Y158F. The 460 nm shoulder, due to the AA, gradually decreases in the presence of 4 mM L-Cth (Figure 1) or 50 mM L-Ser, while a peak centered at 320 nm increases in intensity (Figure 1), with concomitant loss of activity. A similar inactivated 320 nm species was observed for the β-D305N mutant of TrpS following incubation with L-Ser and for several other mutants following reaction with β-chloro-L-alanine (*23*). The model proposed by Ahmed et al. (*23*) to explain the formation of this inactivated 320 nm enzyme form was based on the mechanism of AATase and glutamate decarboxylase inactivation by serine *O*-sulfate (*21*, *22*). In this model (Scheme 4), the AA intermediate dissociates from the PLP. It may then spontaneously hydrolyze to pyruvate and NH_3, due to the open active-site conformation, or it may attack the external aldimine, thereby inactivating the enzyme. The latter must be a slow process as compared to the β-replacement and -elimination reactions, to account for the substantial accumulation of pyruvate, which is most apparent after 60 min as the linear increase in 320 nm absorbance (Figure 1). Following enzyme inactivation and removal of the remaining substrate and pyruvate by dialysis, the pH was adjusted to 11.5, and a PLP derivative with a λ_{max} of 424 nm (**5**, Scheme 4) was observed. Formation of the 424 nm species (**5**, Scheme 4) is diagnostic of the mechanism of enzyme inactivation by the AA intermediate first described for the reaction of AATase with L-serine-*O*-sulfate (*21*, *22*).

While the T85A and Y158F mutants have only small impacts on the β-replacement activity of ytCBS, the results demonstrate that these residues play a role in determining the reaction specificity of the enzyme by maintaining the proper active-site conformation and likely also the equilibrium between the open and the closed forms of the enzyme.

Thr81, and to a Lesser Extent Ser82, Are Key Determinants of the Catalytic Efficiency of ytCBS. Both the β-replacement and the β-elimination activities of the T81A mutant for the substrate L-Ser are very low (Table 2 and Figure 2). The former is reduced by 4 orders of magnitude as compared to the native enzyme, and the reverse reaction is similarly compromised. In the OASS/K41A-L-Met complex, Thr81-Oγ is 2.75 and 3.17 Å from the carboxylate oxygens of L-Met and is 2.69 and 2.83 Å from Ser82-Nα and Gly83-Nα, respectively (Scheme 2). The position of Thr81 in the active site suggests that the role of this residue is to contribute to the maintenance of the correct arrangement of the active-site residues with respect to each other and to the bound substrate. Therefore, although the ratio of 36 for the $k_{cat}^{L-Ser}/K_m^{L-Ser}$ values of the β-replacement and -elimination reactions for T81A (Table 3) suggests a role in reaction specificity, the large reduction in the former activity of this mutant supports a more significant role in catalysis and in maintenance of the required active-site conformation.

The reductions of the K_{mF}^{L-Ser}, k_{catF}/K_{mF}^{L-Ser}, and $K_{d(app)}^{L-Ser}$ values by 21-, 76-, and 67-fold, respectively, for the S82A mutant as compared to ytCBS (Table 2) demonstrate that the side chain hydroxyl group of Ser82 is also involved in L-Ser binding and positioning. However, the rate constant for turnover of L-Ser by β-elimination by the S82A mutant is 2 orders of magnitude greater than that of T81A, and the ratio of $k_{cat}^{L-Ser}/K_m^{L-Ser}$ values for the β-replacement and -elimination reactions is 21 for S82A (Table 2). Therefore, Ser82 is also a determinant of the reaction specificity of ytCBS. Ser82 is conserved in CBS and in all OASS sequences except for that of *S. typhimurium*, where it is asparagine.

Gln157 Controls Partitioning between Reaction Pathways in ytCBS. Nϵ and Oϵ of Gln157 in yCBS are expected to form H-bonds to Oγ of Thr85 in the open and closed (L-Met complex) active-site conformations, respectively (see above and refs *17* and *32*). The former H-bond is conserved in hCBS, where the distance between Gln157-Nϵ and Thr85-Oγ is 2.53 Å (*7*, *8*). In addition, Gln157-Nϵ of the OASS/K41A-L-Met external aldimine is 2.89 and 2.83 Å from the backbone carbonyl oxygen of Pro80 and one of the carboxylate atoms of L-Met (Scheme 2), respectively, in the closed conformation of OASS (*17*). These observations suggest that Gln157 is likely involved in anchoring the carboxylate group of L-Ser and PLP-associated intermediates and in forming contacts involved in loop closure. The three Gln157 mutants provide insight into the role of this residue. The Q157A construct eliminates all of the H-bonds to the side chain of this residue, while Q157E may conserve the Oϵ interactions, and Q157H may retain those formed by Nϵ. The lack of β-replacement activity and detection of the β-elimination activity for the Q157A and Q157E mutants establish that Gln157 is a key determinant of the reaction specificity of yCBS. These results suggest that the closed conformation of the active site is much less favored in these mutants than in wild-type ytCBS. Incubation of Q157A (Figure 3) or Q157E with 50 mM L-Ser results in significant accumulation of pyruvate, as evidenced by the absorbance at <400 nm shown in Figure 3, but $>50\%$ of the PLP

absorbance at 412 nm remains after the 3 h incubation; therefore, this enzyme only rarely undergoes inactivation through covalent attack by AA (Scheme 4). In contrast, incubation of Q157H under the same conditions resulted in much less absorbance due to pyruvate and a shift in the λ_{max} from 412 to 320 nm (Figure 3). Conversion of the 320 nm species to one absorbing at 424 nm, characteristic of **5** (Scheme 4), following an increase in the pH of the reaction to 11.5 argues that, similar to the Y158F mutant, Q157H is inactivated by L-Ser by release and subsequent attack of AA. The observation of this inhibited enzyme form for two of the seven ytCBS mutants investigated suggests that both Gln157 and Tyr158 are key residues for ensuring that the reactive AA intermediate does not inactivate the enzyme. The kinetic parameters for formation of the 320 nm species by the Q157H mutant (k_{max} and K_m^{app} values of $(4.3 \pm 0.4) \times 10^{-4}$ s^{-1} and 35 ± 9 mM, respectively) verify that its formation is very slow and requires very high concentrations of L-Ser. Interestingly, substrate inhibition of the formation of the 320 nm species is observed at >100 mM L-Ser (Figure 5). This result implicates association of a second molecule of L-Ser, likely in the L-Hcys binding site, that permits a rearrangement of the active site and decreases the flux through the inactivation pathway (Scheme 4). Substrate inhibition of wild-type ytCBS has also been noted at >50 mM L-Ser (S. M. Aitken, unpublished results).

ACKNOWLEDGMENT

We thank Dr. Andrew Eliot for incisive comments on the manuscript.

REFERENCES

1. Carson, N. A. J., Dent, C. E., Field, C. M. B., Neill, D. W., Westall, R. G., and Cusworth, D. C. (1963) *Arch. Dis. Child. 38*, 425−436.
2. Mudd, S. H., Laster, L., Finkelstein, J. D., and Irreverre, F. (1964) *Science 143*, 1443−1445.
3. Mudd, S. H., Levy, H. L., and Skovby, F. (1989) in *The Metabolic Basis of Inherited Disease* (Scriver, C. R., Beaudet, A. L., Sly, W. S., and Valle, D., Eds.) pp 693−734, McGraw-Hill, New York.
4. Kraus, J. P., Janosik, M., Kozich, V., Mandell, R., Shih, V., Sperandeo, M. P., Sebastio, G., de Franchis, R., Andria, G., Kluijtmans, L. A., Blom, H., Boers, G. H., Gordon, R. B., Kamoun, P., Tsai, M. Y., Kruger, W. D., Koch, H. G., Ohura, T., and Gaustadnes, M. (1999) *Hum. Mutat. 13*, 362−375.
5. Kery, V., Bukovska, G., and Kraus, J. P. (1994) *J. Biol. Chem. 269*, 25283−25288.
6. Taoka, S., Ohja, S., Shan, X., Kruger, W. D., and Banerjee, R. (1998) *J. Biol. Chem. 273*, 25179−25184.
7. Taoka, S., Lepore, B. W., Kabil, O., Ojha, S., Ringe, D., and Banerjee, R. (2002) *Biochemistry 41*, 10454−10461.
8. Meier, M., Janosik, M., Kery, V., Kraus, J. P., and Burkhard, P. (2001) *Embo J. 20*, 3910−3916.
9. Maclean, K. N., Janosik, M., Oliveriusova, J., Kery, V., and Kraus, J. P. (2000) *J. Inorg. Biochem. 81*, 161−171.
10. Jhee, K. H., McPhie, P., and Miles, E. W. (2000) *J. Biol. Chem. 275*, 11541−11544.
11. Jhee, K. H., Niks, D., McPhie, P., Dunn, M. F., and Miles, E. W. (2001) *Biochemistry 40*, 10873−10880.
12. Taoka, S., and Banerjee, R. (2002) *J. Biol. Chem. 277*, 22421−22425.
13. Aitken, S. M., and Kirsch, J. F. (2003) *Biochemistry 42*, 571−578.
14. Miles, E. W. (2001) *Chem. Rec. 1*, 140−151.
15. Tai, C. H., and Cook, P. F. (2001) *Acc. Chem. Res. 34*, 49−59.
16. Rege, V. D., Kredich, N. M., Tai, C. H., Karsten, W. E., Schnackerz, K. D., and Cook, P. F. (1996) *Biochemistry 35*, 13485−13493.
17. Burkhard, P., Tai, C. H., Ristroph, C. M., Cook, P. F., and Jansonius, J. N. (1999) *J. Mol. Biol. 291*, 941−953.
18. Kashiwamata, S., and Greenberg, D. M. (1970) *Biochim. Biophys. Acta 212*, 488−500.
19. Higuchi, R. (1990) in *PCR Protocols: A Guide to Methods and Applications* (Gelfand, M. A., Sninsky, D. H., and White, J. J., Eds.) pp 177−183, Academic Press, New York.
20. Jhee, K. H., McPhie, P., and Miles, E. W. (2000) *Biochemistry 39*, 10548−10556.
21. Likos, J. J., Ueno, H., Feldhaus, R. W., and Metzler, D. E. (1982) *Biochemistry 21*, 4377−4386.
22. Ueno, H., Likos, J. J., and Metzler, D. E. (1982) *Biochemistry 21*, 4387−4393.
23. Ahmed, S. A., Ruvinov, S. B., Kayastha, A. M., and Miles, E. W. (1991) *J. Biol. Chem. 266*, 21548−21557.
24. Christen, P., and Mehta, P. K. (2001) *Chem. Rec. 1*, 436−447.
25. Kirsch, J. F., Eichele, G., Ford, G. C., Vincent, M. G., Jansonius, J. N., Gehring, H., and Christen, P. (1984) *J. Mol. Biol. 174*, 497−525.
26. Capitani, G., McCarthy, D. L., Gut, H., Grutter, M. G., and Kirsch, J. F. (2002) *J. Biol. Chem. 277*, 47935−47942.
27. Clausen, T., Huber, R., Laber, B., Pohlenz, H. D., and Messerschmidt, A. (1996) *J. Mol. Biol. 262*, 202−224.
28. Clausen, T., Huber, R., Prade, L., Wahl, M. C., and Messerschmidt, A. (1998) *EMBO J. 17*, 6827−6838.
29. Rhee, S., Parris, K. D., Hyde, C. C., Ahmed, S. A., Miles, E. W., and Davies, D. R. (1997) *Biochemistry 36*, 7664−7680.
30. Schirch, V., Shostak, K., Zamora, M., and Guatam-Basak, M. (1991) *J. Biol. Chem. 266*, 759−764.
31. Cook, P. F., Hara, S., Nalabolu, S., and Schnackerz, K. D. (1992) *Biochemistry 31*, 2298−2303.
32. Burkhard, P., Rao, G. S., Hohenester, E., Schnackerz, K. D., Cook, P. F., and Jansonius, J. N. (1998) *J. Mol. Biol. 283*, 121−133.

BI035496M